PERGAMON

Chaos, Solitons and Fractals 11 (2000) 2479–2485

CHAOS
SOLITONS & FRACTALS

www.elsevier.nl/locate/chaos

Penetration rate prediction for percussive drilling via dry friction model

Anton M. Krivtsov [a,b], Marian Wiercigroch [b,*]

[a] *St Petersburg State Technical University, Department of Theoretical Mechanics, Politechnicheskaya Street 29, 195251 St Petersburg, Russian Federation*

[b] *Department of Engineering, University of Aberdeen, Fraser Noble Building, King's College, Aberdeen AB24 3UE, UK*

Abstract

A dynamic model of percussive drilling assuming a dry friction mechanism to explain the experimentally observed drop in penetration rate is presented. The inherent nonlinearity of the discontinuous impact process is modelled as a frictional pair, and this can generate the pattern of the impact forces close to reality. Despite quite radical simplifying assumptions, the model is able do describe the fall of material removal rate for a higher static loading with a good agreement to experimental investigations. © 2000 Elsevier Science Ltd. All rights reserved.

1. Introduction

One of the most fascinating phenomenon met by experimentalists in drilling research is a fall of penetration rate for higher static loads. This is known both in manufacturing and downhole drilling. In manufacturing, for example, considering rotary ultrasonic machining (RUM), the material removal rate (MRR) saturates or even decreases for higher level of static forces. Similarly, an increased weight on bit in downhole drilling does not improve the penetration rates when hard strata is met. In this paper, we will concentrate on the rotary ultrasonic drilling, as we have an ongoing experience in this area, e.g., [8,12].

RUM using diamond impregnated or coated tools is considered one of the most efficient machining method for advanced ceramics. Experimental results have shown that the machining rate obtained from RUM is nearly six–ten times higher than that from conventional grinding process under similar conditions [1]. Since introduction of RUM in the early 1960s by UKAEA, Harwell in England, a lot of experimental studies were performed investigating influences of various working conditions on the RUM efficiency [2–8]. Different workpiece materials including glass, porcelain, ferrite, alumina, and zirconia were examined. As will be seen the increasing quantity of experimental data demands a theoretical model that could satisfactorily explain the phenomena. Several comprehensive analytical models for the estimation of the MRR for ultrasonic machining were proposed by different authors [9–11]. But all these models were considering ultrasonic drilling mainly from the static point of view, ignoring the dynamics of the drilling process. As a result some well-known dynamic features of the RUM, such as decrease in the MRR for higher values of static forces [3–5] have not be properly described. Saha et al. [9] reported satisfactory agreement with the experiment, even showing the fall in the MRR for higher static loads, but this was obtained by additional

* Corresponding author. Tel.: +44-1224-272509; fax: +44-1224-272497.

E-mail addresses: krivtsov@AK5744.spb.edu, krivtsov@abdn.ac.uk (A.M. Krivtsov), m.wiercigroch@eng.abdn.ac.uk (M. Wiercigroch).

0960-0779/00/$ - see front matter © 2000 Elsevier Science Ltd. All rights reserved.
PII: S0960-0779(00)00017-5

empirical power restriction. The first dynamic model of the RUM process was proposed by Wiercigroch et al. [12], where three degrees of freedom impact model was used to simulate the main mechanism occurring in the ultrasonic drilling. The model was able to explain the MRR fall without any additional assumptions, only as a direct corollary of the system dynamics. However, this model does not account for a progressive motion of the drillbit, and hence the MRR was calculated indirectly that possibly produced very jagged form of the theoretical MRR graph. It is thought that a simple dynamics model, considering only the essential process features connected with the excitation dynamics and tool propagation was required, and such a model is presented in the current paper. The proposed model will investigate the influences of the static force and the amplitude of the dynamic force on the MRR, assuming that the drilling resistance is modelled by a dry friction element. In spite of its simplicity the model is able do describe the fall of MRR for higher static loading.

2. Dry friction model

The presented model is shown in Fig. 1, where m is the mass of the tool, $F(t)$ the overall drilling force, $P(\dot{y})$ the resistive force, x the coordinate of the tool's tip, and y is the coordinate of the dry friction element, which represents the progression of the drilling surface. The equation of motion of the mass takes the following form

$$\begin{aligned} x < y \quad &\Rightarrow \quad m\ddot{x} = F(t), \\ x = y \quad &\Rightarrow \quad m\ddot{x} = F(t) - P(\dot{y}), \end{aligned} \tag{1}$$

which depends on the relative position between x and y coordinates. In turn, the equation of motion for the slider can be expressed as

$$\begin{aligned} \dot{x} \geqslant 0 \quad &\Rightarrow \quad y = x, \\ \dot{x} < 0 \quad &\Rightarrow \quad \dot{y} = 0. \end{aligned} \tag{2}$$

For simplicity of the further analysis it was assumed that the overall drilling force $F(t)$ has the form

$$F(t) = A \sin \omega(t - t_0) + B, \tag{3}$$

where A and ω are the amplitude and frequency of harmonic force, B is the static force, t the time, and t_0 is the time constant. The resistive force $P(\dot{y})$ is modelled by the Coulomb dry friction fulfilling the following conditions

$$\begin{aligned} \dot{y} > 0 \quad &\Rightarrow \quad P(\dot{y}) = Q, \\ \dot{y} = 0 \quad &\Rightarrow \quad P(\dot{y}) \leqslant Q, \end{aligned} \tag{4}$$

where Q stands for the modulus of the dry friction force. From the practical viewpoint one may consider that the dry slider progression (MRR) is due to generation of the dynamic impacts, while decelerating the mass. Therefore we can limit our consideration to the case when $F(t) < Q$. From Eqs. (1)–(4) it can be easily deduced that the considered system can be in one of three unique states (see Table 1).

In order to gain some extra flexibility of the analysis, new dimensionless variables and parameters are introduced. Let the dimensionless time be denoted as $\tau = \omega t$, and prime stands for derivation with the dimensionless time. It is worth to note that the resistive coefficient, Q has a distinct value for any drilled material. On the contrary, the amplitude of the harmonic force and the static force can vary, and can be used as control parameters for the drilling process. Hence, let us divide all the drilling forces by the resistive coefficient, Q

$$f(\tau) \stackrel{\text{def}}{=} \frac{F(t)}{Q}, \quad a \stackrel{\text{def}}{=} \frac{A}{Q}, \quad b \stackrel{\text{def}}{=} \frac{B}{Q}. \tag{5}$$

To complete dimentionlising process, coordinates ξ and η are defined as follows

$$\xi \stackrel{\text{def}}{=} \frac{\omega^2 m}{Q} x, \quad \eta \stackrel{\text{def}}{=} \frac{\omega^2 m}{Q} y. \tag{6}$$

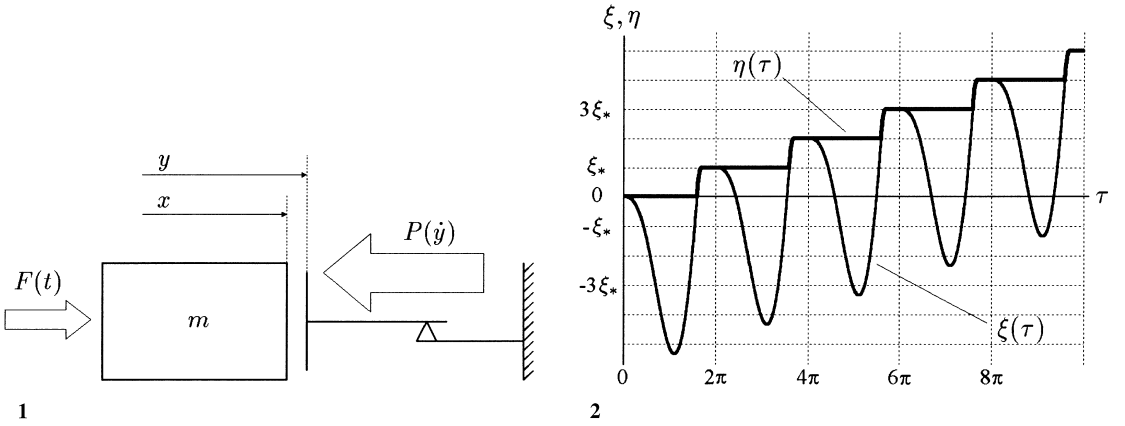

Fig. 1. The dry friction model.
Fig. 2. The progressive stationary motion.

3. Progressive stationary motion

Let us consider a progressive stationary motion, that satisfies the following equations

$$\xi(\tau+2\pi)=\xi_*+\xi(\tau),\quad \eta(\tau+2\pi)=\xi_*+\eta(\tau), \tag{7}$$

where ξ_* is the dimensionless penetration of the drillbit during one excitation period, which is equal to 2π. The time history of the motion of the system is depicted in Fig. 2. The dimensionless MRR calculated per one period is

$$r=\frac{\eta(2\pi)-\eta(0)}{2\pi}=\frac{\xi_*}{2\pi}. \tag{8}$$

If one breaks up one period of the progressive stationary motion into distinct intervals, three sequential time intervals (three stages of the stationary motion) can be specified. They are schematically shown in Fig. 3, and are specified in Table 2. The time intervals α, β and γ satisfy the identity $\alpha+\beta+\gamma=2\pi$. The dimensionless excitation force can be represented in the following form

$$f(\tau)=-a\cos(\tau-\varphi)+b, \tag{9}$$

where $\varphi \overset{\text{def}}{=} \omega t_0-\pi/2$. The sum $\varphi+\pi$ is a phase shift between the overall drilling force and the progressive stationary motion.

The four parameters α, β, γ and φ, specified above, are used to determine the progressive stationary motion. They are unknown and to be found by integrating the equations of motion. The initial conditions to be chosen, are given in Table 3, where $\xi'_-|_{\tau=\alpha}$ and $\xi'_+|_{\tau=\alpha}$ are derivatives calculated in the left and right vicinity of the time when $\tau=\alpha$. There are three different types of the stationary motion, namely motion without stop, motion with stop, and total stop, which are summarized in Table 4. By solving the equations of motion two relations between the parameters α, β and φ of the stationary motion can be obtained

$$a\cos(\alpha-\varphi)-a\cos\varphi-a\alpha\sin\varphi+\frac{1}{2}b\alpha^2=0, \tag{10}$$

Table 1
Three unique states of the system

State	x	y	Condition
Free motion	$m\ddot{x}=F(t)$	$\dot{y}=0$	$x<y$
Drilling	$m\ddot{x}=F(t)-Q$	$y=x$	$\dot{x}>0$
Stop	$\dot{x}=0$	$y=x$	$F(t)\geqslant 0$

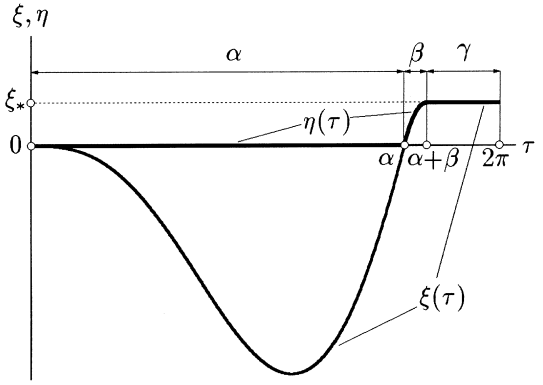

Fig. 3. One period of the motion.

Table 2
Three distinct sequential stages of the stationary

Stage	Time limits	ξ	η
Free motion	$0 < \tau < \alpha$	$\xi'' = f(\tau)$	$\eta = 0$
Drilling	$\alpha < \tau < \alpha + \beta$	$\xi'' = f(\tau) - 1$	$\eta = \xi$
Stop	$\alpha + \beta < \tau < 2\pi$	$\xi = \xi_*$	$\eta = \xi_*$

Table 3
Boundary conditions

Time	Coordinate	Velocity
$\tau = 0$	$\xi = 0$	$\xi' = 0$
$\tau = \alpha$	$\xi = 0$	$\xi'_- = \xi'_+$
$\tau = \alpha + \beta$	–	$\xi' = 0$

Table 4
Three types of the stationary motion

Type	Motion	Conditions
I	No stop	$\alpha + \beta = 0$, $\cos\varphi > b/a$
II	With stop	$\cos\varphi = b/a$, $\sin\varphi > 0$
III	Total stop	$\alpha + \beta = 2\pi$, $b/a > 1$

$$a\sin(\alpha + \beta - \varphi) + a\sin\varphi - b\alpha + (1 - b)\beta = 0. \tag{11}$$

However, to determine all unknowns, one more equation is required, which can be taken from Table 4. For the motion without stop the resulting system of equations can be solved analytically, for the motion with stop, a numeric solution is required. The solution can be essentially simplified in the case of small excitation, when the drilling force is small with respect to resistive force (a, $b \ll 1$). This case is particularly very interesting from a practical point of view. If the motion parameters are found then the dimensionless MRR can be obtained as

$$r = \frac{1}{2\pi}\left(a\cos(\gamma + \varphi) - a\cos(\alpha - \varphi) - a\beta\sin(\gamma + \varphi) + \frac{1}{2}(1 - b)\beta^2\right). \tag{12}$$

For experimental verification purposes it is useful to operate with dimensional MRR, which can be calculated as

$$R = \frac{SQ}{\omega m} r, \tag{13}$$

where S is the cross-section of the drillbit, Q the dry friction coefficient, ω the frequency of the harmonic force and m is the mass of the tool.

4. Results and discussion

Let us examine the influences of the main drilling parameters, A and B on the dynamic system behavior, keeping in mind, that A is the amplitude of the harmonic force and B is the static force.

Relative periods of the free motion, $\alpha/(2\pi)$ and the stop, $\gamma/(2\pi)$ as functions of the drilling forces ratio, B/A are depicted in Fig. 4. Different graphs correspond to different values of the relative excitation amplitude, $a = A/Q$. The highest (thick) graph in both figures corresponds to $a \to 0$ that is the small excitation case. Lower curves are calculated for $a = 0.1,\ 0.2, \ldots, 1.0$ (Fig. 4(a)) and for $a = 0.1,\ 0.2, \ldots, 0.5$ (Fig. 4(b)). Relative drilling period $\beta/(2\pi)$ as a function of B/A is shown in Fig. 5(a). For small excitation β is a small quantity that can be seen as a thick horizontal line in the bottom of Fig. 5(a). Higher curves correspond to $a = 0.1,\ 0.2, \ldots, 0.5$. Parameter φ as a function of the drilling forces ratio, B/A for different values of the relative excitation is shown in Fig. 5(b). We need to remember that $\varphi + \pi$ is the phase shift between the drilling force and the tool motion. The highest (thick) curve in Fig. 5(b) corresponds the small parameters approximation $a \to 0$, where lower curves are calculated for $a = 0.1,\ 0.2, \ldots, 1.0$.

MRR as a function of the relative hydrostatic force, B/A ($A =$ constant) and the relative amplitude of the harmonic force, A/B ($B =$ constant), calculated from Eq. (12) is shown in Fig. 6. Different graphs correspond to varying values of the relative excitation amplitude, $a = A/Q$ for Fig. 6(a), and to different values of the relative hydrostatic force, $b = B/Q$ as depicted in Fig. 6(b). The lowest (thick) curve in both figures corresponds to the small excitation case $a \to 0$ or $b \to 0$. In Fig. 6(a) higher curves are calculated for $a = 0.1,\ 0.2, \ldots, 0.5$. In Fig. 6(b) higher curves correspond to $b = 0.05,\ 0.10, \ldots, 0.25$.

Now consider Fig. 6(a), the case of small excitation (lower thick curve). The relationship between the MRR and the static force B has a clearly pronounced maximum as indicated earlier [12]. The shape of the MRR graphs is in good agreement with MRR relations obtained from experiments [3–5]. It can be seen that the MRR increases in the region of the motion without stop, and it reaches its maximum value in the region of the motion with stop at $B/A \approx 0.4$. However, one needs to note that the maximum is close to the border between these two regions, which is indicated in Fig. 6(a) by a dashed vertical line at $B/A \approx 0.3$. For the further increase of B/A the MRR decreases down to zero at $B = A$. The maximum value of the MRR for the small excitation is

$$R_{\max} = \frac{SA^2}{\omega m Q} p_{\max}, \tag{14}$$

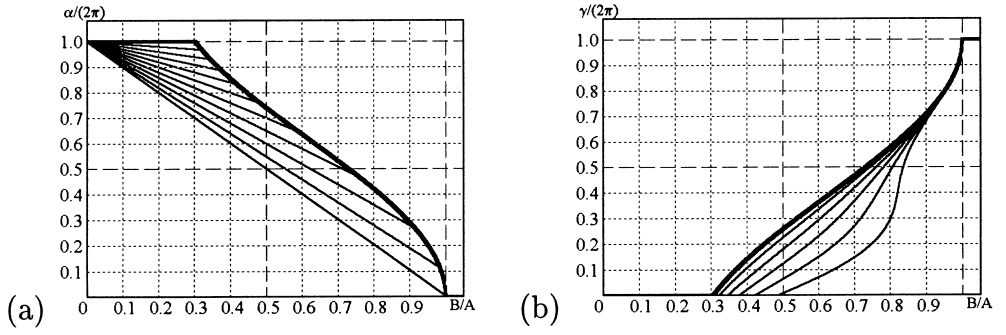

Fig. 4. Free motion period $\alpha/(2\pi)$ and stop period $\gamma/(2\pi)$ as functions of the drilling forces ratio B/A for different values of the relative excitation amplitude $a = A/Q$.

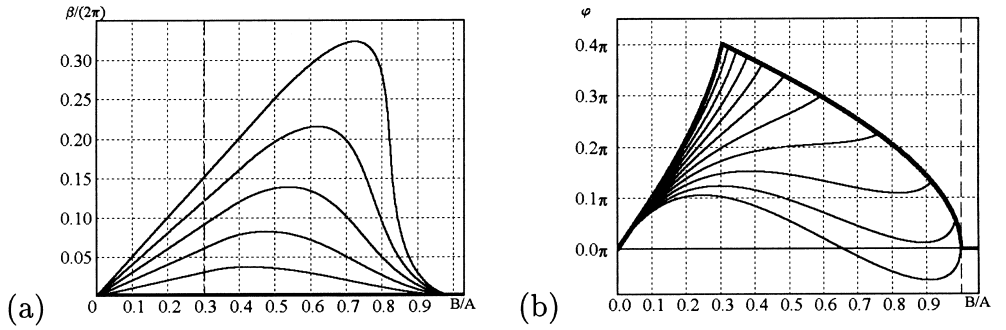

Fig. 5. Drilling period $\beta/(2\pi)$ and phase shift φ as functions of the drilling forces ratio B/A for different values of the relative excitation amplitude $a = A/Q$.

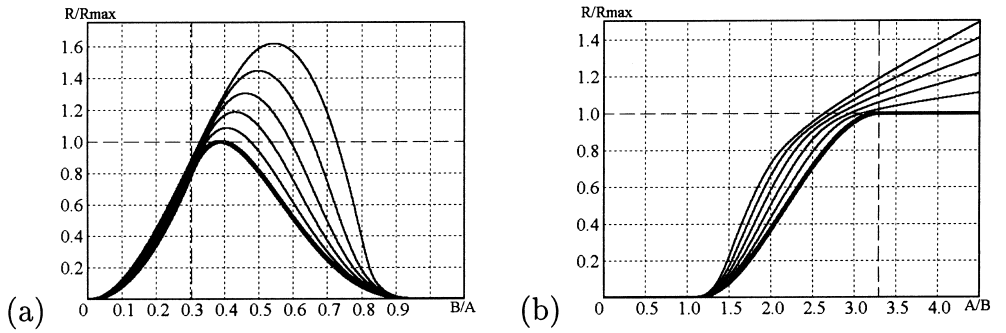

Fig. 6. MRR as functions of the relative hydrostatic force B/A (A = constant) and the relative amplitude of the harmonic force A/B (B = constant).

where $p_{\max} \approx 0.360$. The higher curves in the Fig. 6(a) correspond to nonsmall excitation and they are shown as a ratio to the small excitation value of $R_{\max}$ (Eq. (14)).

Now we will investigate the influence of the amplitude of the harmonic force A on the MRR while the static force B is kept constant; in the case of the small excitation – see Fig. 6(b) (lower thick graph). The MRR is equal to zero for $A \leqslant B$, then it increases monotonically in the region of the motion with stop, and has constant value in the region of the motion without stop $A/B > \sqrt{1+\pi^2} \approx 3.3$. Hence, in the small excitation case there is no need to increase the amplitude of harmonic force more than $3.3B$ (see dashed vertical line in Fig. 6(a)). The maximum value of the MRR can be calculated from

$$R_{\max} = \pi \frac{SB^2}{\omega m Q}. \tag{15}$$

The higher curves in the Fig. 6(b) correspond to nonsmall excitation and they are shown as a ratio to the small excitation value of $R_{\max}$ (Eq. (15)). For nonsmall excitation the MRR is a monotonic function of the excitation amplitude, b. It is worth to note that for a bigger excitation, the MRR does not have the horizontal region, and inclination of this part of the curve is greater for greater values of b.

5. Concluding remarks

The developed model allows to calculate the material removal rate R in the form

$$R = \frac{SQ}{\omega m} r\left(\frac{A}{Q}, \frac{B}{Q}\right), \tag{16}$$

where S is the cross-section of the drillbit, Q the resistive force of the material, ω the frequency of harmonic force, m the tool mass, and A and B are the controllable parameters of the drilling force; $r = r(a, b)$ is a known function of two variables.

An investigation of the MRR function given by Eq. (16) provides the following conclusions.

1. Drilling action is only possible if the static force is smaller than the amplitude of the harmonic force, $B < A$. If B is greater than A the drillbit is motionless.
2. The MRR function of the static force, B (while A is kept constant) has a well-pronounced maximum, which is taken at $B \approx 0.39A$ for a small excitation and shifts to the right for greater excitation.
3. The MRR is monotonically increasing function of the amplitude of the harmonic force, A. In the case of the small excitation this function becomes constant for $A/B > \sqrt{1+\pi^2}$, which means that an increase in the amplitude more then approximately $3.3B$ has no effect.

Acknowledgements

The authors would like to kindly acknowledge the financial support from the Royal Society of London under the grant No. NATO/98/nvb funded jointly by NATO and the Royal Society.

References

[1] Pei ZJ, Khanna N, Ferreira PM. Rotary ultrasonic machining of structural ceramics – a review. Ceram Eng Sci Proc 1995;16(1):259–78.
[2] Markov AI, Ustinov ID. A study of the ultrasonic diamond drilling of non-metallic materials. Ind Diamond Rev March 1972; 97.
[3] Markov AI. Ultrasonic machining of materials. Mashinostroenie, Moscow, 1980 (in Russian).
[4] Petrukha PG. Ultrasonic diamond drilling of deep holes in brittle materials. Russian Eng J L 1980:71.
[5] Kubota M, Tamura J, Shimamura N. Ultrasonic machining with diamond impregnated tools. Precision Eng 1977;11:127.
[6] Komaraiah M, Mannan MP, Reddy-Narasimha PN, Victor S. Investigation of surface roughness and accuracy of ultrasonic machining. Precision Eng 1988;10:58.
[7] Prabhakar D, Ferreira PM, Haselkorn M. An Experimental investigation of material removal rates in rotary ultrasonic machining. Trans North American Manufact Res Inst SME 1992;99:211–8.
[8] Wiercigroch M, Neilson RD, Player MA, Barber H. Experimental study of rotary ultrasonic machining: dynamic aspects. Mach Vibrat 1993;2:187–97.
[9] Saha J, Bhattacharyya A, Mishra PK. Estimation of material removal rate in USM process: a theoretical and experimental study. In: Proceedings of the 27th MATADOR Conference. UMIST, Manchester, April 1988:275.
[10] Prabhakar D, Pei ZJ, Ferreira PM, Haselkorn M. A theoretical model for predicting material removal rates in rotary ultrasonic machining of ceramics. Trans North American Manufact Res Inst SME 1993;21:167–72.
[11] Pei ZJ, Prabhakar D, Ferreira PM, Haselkorn M. A mechanistic approach to the prediction of material removal rates in rotary ultrasonic machining. Trans ASME, J Eng Ind 1995;117:142–51.
[12] Wiercigroch M, Neilson RD, Player MA. Material removal rate prediction for ultrasonic drilling of hard materials using an impact oscillator approach. Phys Lett A 1999;259(2):91–6.